

Interaction of Lysine Dendrimers of 2nd and 3rd Generation with Stack of Amyloid Peptides. Molecular Dynamics Simulation.

I. Neelov, E. Popova, D. Khamidova and F. Komilov

Abstract—In present paper, molecular dynamics simulation is used to study amyloid fibril destruction by oppositely charged dendrimers of second and third generation. Dendrimers are often used for delivery of drugs and biological molecules. They also could be used as antibacterial, antiviral and anti-amyloid agents. Since lysine dendrimers are less toxic than conventional synthetic dendrimers, they were chosen for present study and systems consisting of 2nd and 3rd generation dendrimers and stack of 16 short amyloid peptides in water were studied. It was shown that lysine dendrimers of both generations destroy amyloid stack and form stable complexes with amyloid peptides. The structures of the complexes in equilibrium state were investigated. Also it was obtained that peptides in complexes stay mainly on the surface of dendrimer and do not penetrate into them. The results obtained in present paper could be useful for elaboration in future the anti-amyloid agents for treatment of Alzheimer's disease, since it is believed that one of the reasons for its occurrence is the formation of amyloid fibrils.

Keywords—lysine dendrimers, amyloid fibrils, computer simulation, molecular dynamics method

I. INTRODUCTION

ALZHEIMER'S disease is currently one of the most common incurable neurodegenerative diseases. It is characterized by accumulation of amyloid plaques formed by amyloid A β peptides in brain tissues [1, 2]. Diagnostics of Alzheimer's disease is an extremely difficult task even with the most modern methods and devices. Its primary symptoms begin long before the appearance of serious pathologies and often coincide with symptoms of other nervous system diseases. In treatment of this disease three types of drugs are used: cholinesterase inhibitors (Galantamine, Donepezil and their analogues); drugs that reduce the activity of the glutamate mediator (Memantine); antipsychotic drugs for psychosis and

This work was supported by grant of the Government of Russian Federation 074-U01 and by RFBR grant 16-03-00775.

F. I. Neelov is with ITMO University and Institute of Macromolecule Compounds, St. Petersburg, Russia (corresponding author to provide phone: +7-962 7207977; e-mail: i.neelov@mail.ru).

S. E. Popova is with ITMO University, St. Petersburg, Russia. She is also with the Research Institute of Hygiene, Occupational Pathology and Human Ecology, St. Petersburg, Russia (e-mail: arabka2008@mail.ru).

T. D. Khamidova is with Tajik National University, Dushanbe, 734025, Tajikistan (e-mail: deya757@mail.ru).

F. F. Komilov is with Tajik National University, Dushanbe, 734025, Tajikistan (e-mail: komfaiz@mail.ru)

aggression suppressing. This disease in the early stages causes short-term memory disorders, and later leads to long-term memory disorders, speech and cognitive impairment, and ultimately leads to death. Inhibition of beta-amyloid aggregation is one of the most promising ways of disease control.

Dendrimers are branched polymers that are widely used in industrial and biomedical applications. They were used as drug and gene delivery systems, as a branched carrier for multiple antigen peptides (MAPs), as antiviral and antibacterial agents. It was experimentally shown that dendrimers can destroy amyloid fibrils [3]. Lysine dendrimers are important class of dendrimers consisting of lysine amino acid residues as branching repeating units. Recently it was shown that lysine dendrimers also could destroy amyloid fibrils [4].

The goal of present paper is to study the interaction of lysine dendrimers of different generations and stack of amyloid peptides in order to understand the mechanism responsible for amyloid fibrils destruction by dendrimer.

II. METHODS AND MATERIALS

A. Molecular dynamics method

Molecular dynamics (MD) method is currently the main method for simulation of polymer and biopolymer systems. The method consists in numerical solution of the classical Newton equations of motion for all atoms of the all molecules in the system:

$$F_i = m_i \frac{d^2 r_i(t)}{dt^2} \quad (1)$$

MD is used for detailed study of many specific molecules using both detailed full-atomic models as well as more general coarse-grained models. The potential energy of these models usually include valence bonds, valence angles and dihedral angle energies as well as van der Waals and electrostatic energies. The definition of parameters set adequately describing the test molecule properties (force-field) is challenging and requires the experimental data for these molecules, quantum chemical calculations as well as iterative procedures and a very large amount of machine time. These calculations can be made only by large groups of specialists. Due to this reason several packages of standard computer programs, in which these parameters are defined for a fairly

wide range of molecules become widely used in recent years. Currently the most popular molecular modeling packages are GROMACS, AMBER, CHARMM, and some others. Our simulation was performed by molecular dynamics method using the GROMACS 4.5.6 software package [5] and one of the most modern AMBER_99SB-ildn force fields [6].

B. Model and Calculation Method

Modeling was performed using the molecular dynamics method for systems consisting of one lysine dendrimer of second or third generation with 16 or 32 positively charged NH_3^+ end groups, 16 LVFFAE peptides, water molecules and chlorine counterions in a cubic cell with periodic boundary conditions. The initial conformation for peptide with internal rotation angles of $\varphi = -135^\circ$, $\psi = 135^\circ$, $\theta = 180^\circ$ was modelled by Avogadro chemical editor. The structures were optimized in vacuum using molecular mechanics of AMBER force field. Further energy minimizations and simulations were performed using the GROMACS 4.5.6 software package and AMBER_99SB-ildn force fields. The potential energy of this force field consists of valence bonds and angles deformation energy, internal rotation angles, van der Waals and electrostatic interactions. The procedure of molecular dynamics simulation used for lysine dendrimers and polyelectrolytes has been described earlier in [7-34]. In all calculations the normal conditions (temperature 300 K, pressure 1 ATM) were used. Computing resources on supercomputers "Lomonosov" were provided by supercomputer centre of Moscow State University [35].

The size of dendrimer and complexes at time t was evaluated by the mean square radius of gyration $R_g(t)$ which is defined from:

$$R_g^2(t) = \frac{1}{M} \times \left[\sum_{i=1}^N m_i \times |r_i(t) - R|^2 \right] \quad (2)$$

where R – is the center of mass of subsystem, r_i и m_i – coordinates and masses of i -atom correspondingly, N – is the total number of atoms in subsystem, M is the total mass of dendrimer. This function was calculated using g_gyrate function of GROMACS software.

Radial distribution of density $p(r)$ of atoms in dendrimer and complexes as well as distribution of ion pairs were calculated using g_rdf function of the GROMACS package.

To calculate the coefficient of translational mobility of dendrimer and complexes, the time dependence of the mean square displacements of the centers of inertia (MSD) of corresponding sub-system, were calculated. MSD was calculated using g_msd function of GROMACS.

III. RESULTS AND DISCUSSION

Snapshots of systems consisting of dendrimer, peptides, ions and water during simulation are shown on Fig. 1 (water molecules are not shown for clarity). It is clearly seen that at the beginning of process (Fig. 1, a, d) peptide molecules are rather far from dendrimer. After 30 ns (Fig. 1, b, e) some part of peptide molecules are already adsorbed on the surface of dendrimer, and in the end after 160 ns (Fig. 1, c, f) all peptide molecules in the systems are on its surface. Atoms of dendrimer molecule is shown as beads with diameter equal to their van der Waals radii. Valence bonds of various peptides are shown with lines of different colors (backbone of each peptide is shown by thick line of the same color as valence bonds).

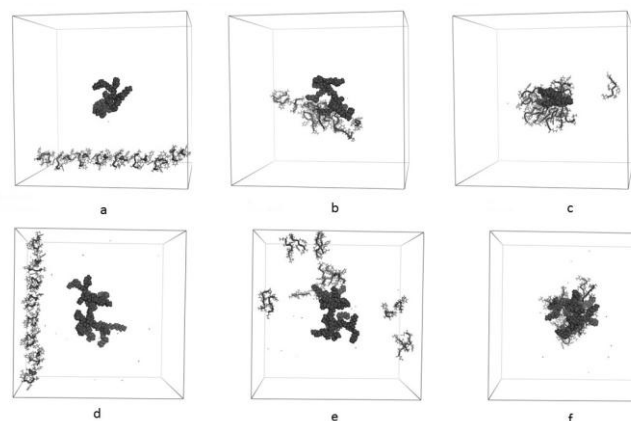


Fig. 1. Stages of the destruction of amyloid stack by G2 and G3 dendrimers and dendrimer-peptides complex formation (initial, intermediate and final): system of G2 dendrimer and 16 peptides at $t = 0$ (a), $t = 20$ ns (b), $t = 160$ ns (c); system of G3 dendrimer and 16 peptides at $t = 0$ (d), $t = 20$ ns (e), $t = 160$ ns (f)

$$\left\langle \sum_t \Delta r^2(t + k\Delta t) \right\rangle = \left\langle \sum_t (r(t + k\Delta t) - r(t))^2 \right\rangle = 6Dt \quad (3)$$

A. Destruction of stack of amyloid peptides by dendrimer and dendrimer-peptide complex formation

First part ($t < 30-40$ ns) of time dependence of gyration radius R_g describes the process of destruction of amyloid stack by G2 and G3 dendrimer and dendrimer-peptides complex formation (Fig. 2). From Fig. 2a it can be seen that 2nd generation dendrimer forms complex with 16 peptides within 20 ns. From Fig. 2b it can be seen that 3rd generation dendrimer forms complex with 16 peptides within 40 ns. After that the complex size R_g fluctuate slightly, but its average values practically do not change with time. Therefore, we can assume that after 40 ns the system is in equilibrium state.

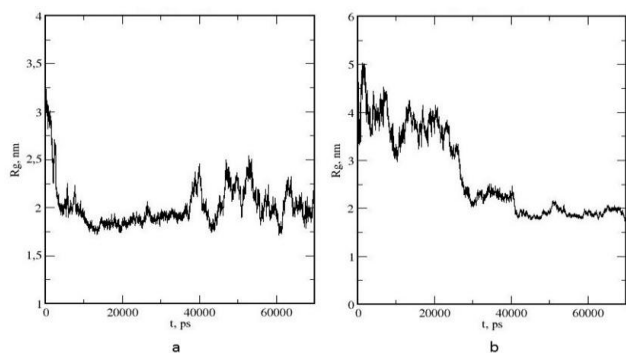


Fig. 2. Time dependence of gyration radius of dendrimer-peptides subsystem during destruction of amyloid stack and dendrimer-peptides complex formation: 1 – G2 and 16 LVFFAE; 2 – G3 and 16 LVFFAE

Another quantity that can characterize the rate of amyloid stack destruction by dendrimer and complex formation is the total number of hydrogen bonds (N) between dendrimer and peptides. The dependence of this value on time is shown on Fig. 3 and demonstrates how the number of contacts between dendrimer and peptides increases during stack destruction and complex formation. This value was calculated using `g_hbonds` function from package of GROMACS.

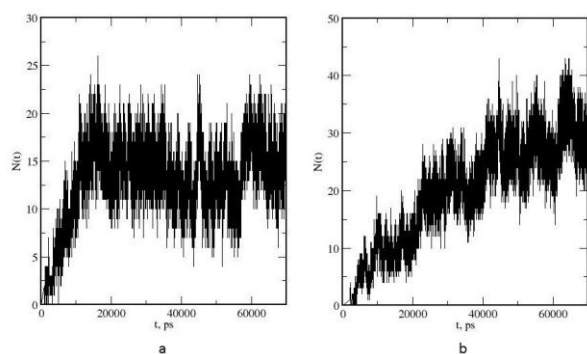


Fig. 3. Time dependence of dendrimer-peptides hydrogen bond number (N) during destruction of amyloid stack and dendrimer-peptides complex formation: 1 – G2 and 16 LVFFAE; 2 – G3 and 16 LVFFAE

From Fig. 3 it can be concluded that first system reaches equilibrium (plateau) after 20 ns and second system reaches equilibrium after 40-50 ns. It correlates with the results of the inertia radii balance obtained in Fig. 2. The number of hydrogen bonds between peptides and dendrimers in equilibrium state shows how tightly peptides associate with dendrimer. The average hydrogen bonds number in equilibrium state ($t > 50$ ns) for the first complex is 14 and for the second complex is equal to 29.

The distance between neighboring peptides in amyloid stack is important characteristic of stability of the stack. This

value also allow to estimate the rate of dendrimer-peptides complex formation after stack was destructed by dendrimer. (Fig.4). In particular during the stack destruction and complex formation with G2 dendrimer, the distance between peptides for the first 40 ns increases. After 40 ns the function fluctuates slightly. It means that interaction with complex is not tightly enough and peptides can return to the stack. In second case (G3 and peptides), at the beginning, there is a large increase in distances between the neighboring peptides of the stack. It means that at small times ($0 < t < 20$ ns) the destruction of amyloid stack occurs and peptides became separated from each other. After 20 ns this separated peptides become attracted by dendrimer and distance between them start to decrease.

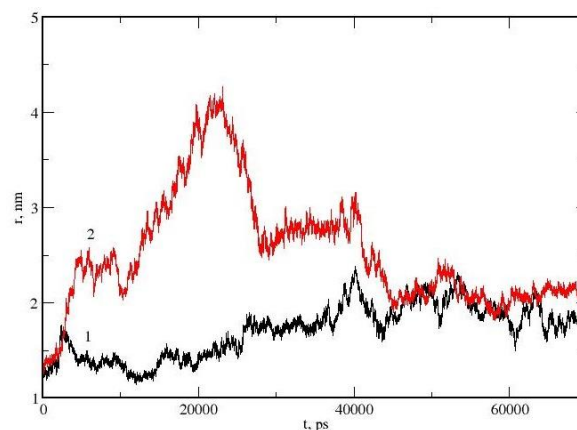


Fig. 4. Changes in distances between amyloid peptides during destruction of amyloid stack and dendrimer-peptides complex formation: 1 – G2 and 16 LVFFAE; 2 – G3 and 16 LVFFAE.

Similar information could be obtained from time dependence of distance between dendrimer and peptides (Fig.5). This value is characterize mainly not state of peptide stack but state of dendrimer-peptide complex. In the beginning of time all peptides are far from dendrimer (see Fig.1). In case of G2 and 16 LVFFAE the peptides are attracted by dendrimer in 20 ns.

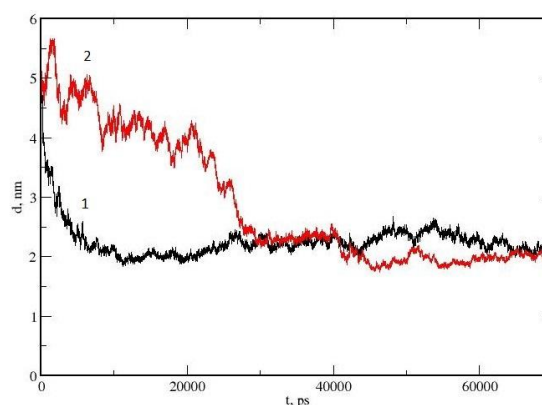


Fig. 5. Changes in distances between dendrimer and peptides during destruction of amyloid stack and dendrimer-peptides complex formation: 1 – G2 and 16 LVFFAE; 2 – G3 and 16 LVFFAE.

In the second case at times less 40-50ns peptides become attracted by oppositely charged dendrimer and distance between dendrimer and peptides decrease. After that the distance does not change further with time. It means that we obtained equilibrium dendrimer-peptides complex at time $t > 40-50$ ns.

B. Modelling of equilibrium state of dendrimer-peptide complex

In equilibrium state the meansquared radius of gyration R_g (averaged through equilibrium part of trajectory) of the first complex (G2 and 16 LVFFAE) is 1.7 times larger, than the size of the dendrimer G3. The meansquared radius of gyration R_g of the second complex (G3 and 16 LVFFAE) is 1.3 times larger, than the size of the dendrimer G3 (Tab. 1). It is quite natural, since it correlates with the molecular weight of the complexes increase compared to the molecular weight of the individual dendrimer. The shape of both complexes can be characterized by their tensor of inertia main component ratio (R_g^{11} , R_g^{22} , R_g^{33}), that are in Tab. 1. For example, in the simplest case, anisotropy can be characterized by ratio R_g^{33} / R_g^{11} . This ratio for second generation dendrimer is 1.69, for third generation dendrimer is 1.35, for the complex of G2 dendrimer with 16 peptides is 1.45 and for the complex of G3 dendrimer with 16 peptides is 1.32. Thus, an addition of peptides practically does not change the anisotropy of our complex comparing to the anisotropy of the initial dendrimer.

Table 1. Eigenvalues R_g^{11} , R_g^{22} , R_g^{33} of tensor of inertia in dendrimer and dendrimer - peptide complex

System	R_g^{11} , nm	R_g^{22} , nm	R_g^{33} , nm	R_g , nm
Dendrimer (G2)	0,64	0,97	1,08	1,12
Dendrimer (G3)	0,98	1,22	1,32	1,44
G2 and 16 LVFFAE	1,26	1,78	1,83	1,98
G3 and 16 LVFFAE	1,25	1,58	1,65	1,85

The distribution function $p(R_g)$ of gyration radius R_g gives more detailed information about fluctuations of R_g of dendrimers-peptides complexes. This function is shown in Fig. 6.

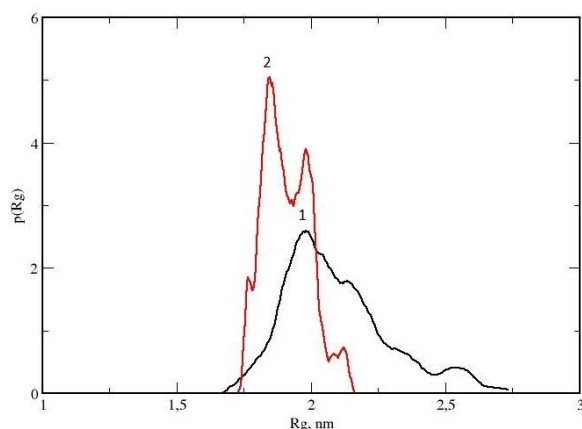


Fig. 6. Distribution function $p(R_g)$ of gyration radius R_g : 1 – G2 and 16 LVFFAE, 2 – G3 and 16 LVFFAE

Information about the internal structure of the equilibrium complex could be obtained using radial density distribution of different groups of atoms relatively center of inertia both for the complexes themselves and for their individual components (Fig. 7).

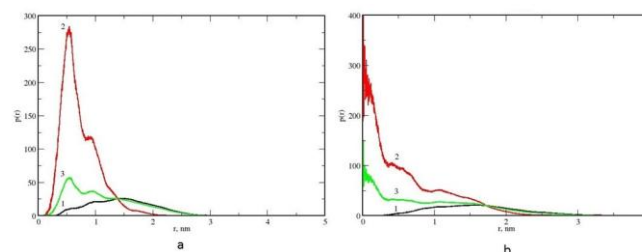


Fig. 7. Radial distribution $p(r)$ density of complexes G2 and 16 peptides (a); G3 and 16 peptides (b). Distribution curves: peptide atoms (1); dendrimer atoms (2); all atoms of complex (3)

The data demonstrates that in both subsystems dendrimer (curve 2) is located in the center of the complex and peptides (curve 1) are mainly on the surface of complex. At the same time, some fraction of peptides could slightly penetrate into outer part of dendrimer.

The distribution function $P(N)$ for the complexes (Fig. 8) has a peak of numbers of bonds that is close to the average value equal to 14 (Fig. 8a) and to 29 (Fig. 8b) and is quite symmetrical. Fluctuations in hydrogen bonds number are for the first system in the range of 6-26 and for the second system in the range of 15-45.

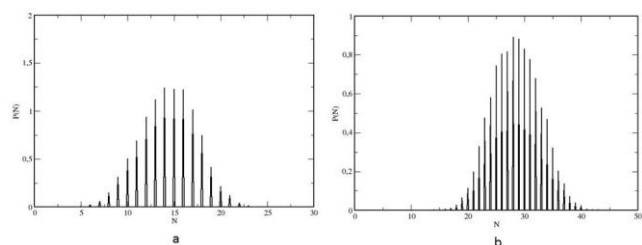


Fig. 8. The distribution function $P(N)$ of hydrogen bonds number N of complex: a – G2 and 16 LVFFAE, b – G3 and 16 LVFFAE

The other characteristic of interaction between dendrimer and peptides (1) in equilibrium dendrimer-peptide complex is the distribution of ion pairs number between their oppositely charged groups. Fig. 9 shows the dependence of ion pairs number on the corresponding distance between pairs of charges of dendrimer and peptides in our complex.

It is seen that there is very sharp peak in both cases, at the distance corresponding to the direct contact between positively charged groups (NH_3^+) of dendrimer and negatively charged groups (COO^-) of the glutamic acid in peptides (Fig 9, curves 1&2). At the same time, NH_3^+ groups of dendrimer form much fewer ion pairs with chlorine ions Cl^- (Fig 9, curves 3&4).

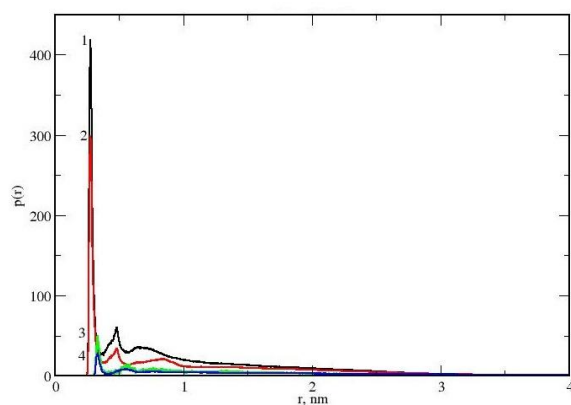


Fig. 9. Radial distribution function of ion pairs: 1 — complex of G2+16 LVFFAE, NH_3^+ groups of dendrimer and peptides COO^- ; 2 – complex of G3+16 LVFFAE, NH_3^+ groups of dendrimer and peptides COO^- ; 3 - complex of G2+16 LVFFAE, NH_3^+ groups of dendrimer and Cl^- ions; 4 - complex of G3+16 LVFFAE, NH_3^+ groups of dendrimer and Cl^- ions

To evaluate the translational mobility of our complex, the time dependence of the mean square displacement of the center of inertia (MSD), was calculated (Fig. 10). MSD was calculated using `g_msd` function of GROMACS. Coefficient of translational diffusion of the complex was obtained from the slope of this time dependence and was equal to $(0,13(1) \pm 0,04) \times 10^5 \text{ sm}^2/\text{s}$ and $(0,14(5) \pm 0,02) \times 10^5 \text{ sm}^2/\text{s}$.

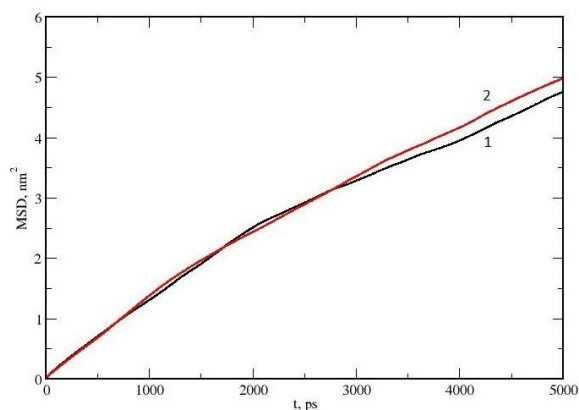


Fig. 10. Mean square displacement of the center of inertia: 1 - complex of G2 and 16 LVFFAE; 2 - G3 and 16 LVFFAE

IV. CONCLUSION

The process of destruction of the stack consisting of 16 amyloid peptides LVFFAE (with charge of each peptide equal -1) by an oppositely charged lysine dendrimers of the second and third generation (having charge equal to 16 and 32), the complex formation and the structure of final equilibrium complex were studied. It was shown that the amyloid fibrils

can be destroyed in 20–40 ns, and stable dendrimer-peptide complexes can be formed after 30–50ns in both cases.

The radial distribution function of atoms number shows that dendrimers are located in the center of the complexes and peptides are mainly on their surfaces. The strong electrostatic interactions between dendrimers and peptides in our complexes (contact of positively charged NH_3^+ groups of dendrimer and carboxyl groups of glutamic acid in peptides) were demonstrated. At the same time, we found that NH_3^+ groups of dendrimers form much fewer ion pairs with chlorine ions Cl^- .

ACKNOWLEDGMENT

This work was supported by grants of the Russian Federation Government 074-U01 and RFBR 16-03-00775. The research was prepared using resources of Supercomputer Center of Lomonosov Moscow State University.

REFERENCES

- [1] A.T. Petkova, W.M. Yau, R. Tycko, "Experimental Constraints on Quaternary Structure in Alzheimer's β -Amyloid Fibrils". *Biochemistry*, vol. 45, 2006, pp. 498–512.
- [2] A.K. Paravastu, R.D. Leapman, W.M. Yau, R. Tycko, "Molecular Structural Basis for Polymorphism in Alzheimer's β -Amyloid Fibrils". *Proc. Natl. Acad. Sci. U.S.A.*, vol. 105, 2008, pp. 18349–18354.
- [3] B. Klajnert, M. Bryszewska, J. Cladera, "Molecular Interactions of Dendrimers with Amyloid Peptides: pH Dependence". *Biomacromolecules*, vol. 7, 2006, pp. 2186–2191.
- [4] I.M. Neelov, A. Janaszewska, B. Klajnert, M. Bryszewska, N. Makova, D. Hicks, H. Pearson, G.P. Vlasov, M.Yu. Ilyash, D.S. Vasilev, N.M. Dubrovskaya, N.L. Tumanova, I.A. Zhuravin, A.J. Turner, N.N. Nalivaeva, "Molecular properties of lysine dendrimers and their interactions with $\alpha\beta$ -peptides and neuronal cells". *Current Medical Chemistry*, vol. 20, 2013, pp. 134–143.
- [5] B. Hess, C. Kutzner, D. Van Der Spoel, E. Lindahl, "GROMACS 4: Algorithms for highly efficient, load-balanced, and scalable molecular simulation". *Journal of Chemical Theory and Computation*, vol. 4, 2008, pp. 435–447.
- [6] V. Hornak, R. Abel, A. Okur, D. Strockbine, A. Roitberg, C. Simmerling, "Comparison of multiple amber force fields and development of improved protein backbone parameters". *Proteins: Structure Function and Genetics*, vol. 65, 2006, pp. 712–725.
- [7] A. Darinskii, Y. Gotlib, M. Lukyanov, I. Neelov, "Computer simulation of the molecular motion in LC and oriented polymers". *Progr. Colloid & Polym. Sci.*, vol. 91, 1993, pp.13-15.
- [8] A.A. Darinskii, Y.Y. Gotlib, A.V. Lyulin, I.M. Neelov, "Computer modeling of polymer chain local dynamics in a field of a liquid crystal type". *Vysokomolec. Soed. Ser. A*, vol. 33, 1991, pp.1211-1220.
- [9] A. Darinskii, A. Lyulin, I. Neelov, "Computer simulations of molecular motion in liquid crystals by the method of Brownian dynamics". *Macromol.Theory & Simulation*, vol. 2, 1993, pp. 523-530.
- [10] J. Ennari, M. Elomaa, I. Neelov, F. Sundholm, "Modelling of water free and water containing solid polyelectrolytes". *Polymer*, vol. 41, 2000, pp. 985-990.
- [11] J. Ennari, I. Neelov, F. Sundholm, "Comparison of Cell Multipole and Ewald Summation Methods for Solid Polyelectrolyte". *Polymer*, vol. 41, 2000, pp. 2149-2155.
- [12] J. Ennari, I. Neelov, F. Sundholm, "Molecular Dynamics Simulation of the PEO Sulfonic Acid Anion in Water". *Comput Theor Polym Sci.*, vol. 10, 2000, pp. 403-410.
- [13] J. Ennari, I. Neelov, F. Sundholm, "Molecular dynamics simulation of the structure of PEO based solid polymer electrolytes". *Polymer*, vol. 41, 2000, pp. 4057-4063.

- [14] J. Ennari, I. Neelov, F. Sundholm, "Estimation of the ion conductivity of a PEO-based polyelectrolyte system by molecular modeling". *Polymer*, vol. 42, 2001, pp. 8043–8050.
- [15] J. Ennari, I. Neelov, F. Sundholm, "Modelling of gas transport properties of polymer electrolytes containing various amount of water". *Polymer*, vol. 45, 2004, pp. 4171–4179.
- [16] I.M. Neelov, D.B. Adolf, A.V. Lyulin, G.R. Davies, "Brownian dynamics simulation of linear polymers under elongational flow: Bead-rod model with hydrodynamic interactions". *Journal of Chemical Physics*, vol. 117, 2002, pp.4030-4041.
- [17] I.M. Neelov, D.B. Adolf, "Brownian Dynamics Simulation of Hyperbranched Polymers under Elongational Flow". *J. Phys. Chem. B.*, vol. 108, 2004, pp. 7627-7636.
- [18] I.M. Neelov, D.B. Adolf, "Brownian Dynamics Simulations of Dendrimers under Elongational Flow: Bead-Rod Model with Hydrodynamic Interactions". *Macromolecules*, vol. 36, 2003, pp. 6914-6924.
- [19] P.F. Sheridan, D.B. Adolf, A.V. Lyulin, I. Neelov, G.R. Davies, "Computer simulations of hyperbranched polymers: The influence of the Wiener index on the intrinsic viscosity and radius of gyration". *Journal of Chemical Physics*, vol. 117, 2002, pp. 7802-7812.
- [20] M.A. Mazo, M.Y. Shamaev, N.K. Balabaev, et al. "Conformational mobility of carbosilane dendrimer: Molecular dynamics simulation". *Physical Chemistry and Chemical Physics*, vol. 6, 2004, pp. 1285-1289.
- [21] I.M. Neelov, D.B. Adolf, T.C.B. McLeish, E. Paci. "Molecular Dynamics Simulation of Dextran Extension by Constant Force in Single Molecule AFM". *Biophysical J.*, vol. 91, 2006, pp. 3579–3588.
- [22] I.M. Neelov, D.A. Markelov, S.G. Falkovich, M.Yu. Ilyash., B.M. Okrugin, A.A. Darinskii, "Mathematical modeling of lysine dendrimers. Temperature dependencies". *Vysokomolec. Soed. Ser. A* , vol. 55, 2013, pp. 963–970.
- [23] S. Falkovich, D. Markelov, I. Neelov, A. Darinskii, "Are structural properties of dendrimers sensitive to the symmetry of branching? Computer simulation of lysine dendrimers". *Journal of Chemical Physics*, vol. 139, 2013, pp. 064903.
- [24] I. Neelov, S. Falkovich, D. Markelov, E. Paci, A. Darinskii, H. Tenhu, "Molecular dynamics of lysine dendrimers. Computer simulation and NMR", In: *Dendrimers in Biomedical Applications*, Eds. London: Royal Society of Chemistry, 2013, pp. 99–114.
- [25] I.M. Neelov, A.A. Mistonova, A.Yu. Khvatov, V.V. Bezrodny, "Molecular dynamics simulation of peptide polyelectrolytes". *Scientific and Technical Journal of Information Technologies, Mechanics and Optics*, vol. 4, 2014, pp. 169–175.
- [26] E.V. Popova, O.V. Shavykin, I.M. Neelov, F. Leermakers, "Molecular dynamics simulation of lysine dendrimer and Semax peptides interaction", *Scientific and Technical Journal of Information Technologies, Mechanics and Optics*, vol. 4, 2016, pp. 716–724.
- [27] O.V. Shavykin, E.V. Popova, A.A. Darinskii, I.M. Neelov, F. Leermakers, "Computer simulation of local mobility in dendrimers with asymmetric branching by brownian dynamics method". *Scientific and Technical Journal of Information Technologies, Mechanics and Optics*, vol.16, 2016, pp. 893-902.
- [28] M.Yu. Ilyash, D.N. Khamidova, B.M. Okrugin, I.M. Neelov, "Computer Simulation of Lysine Dendrimers and their Interactions with Amyloid Peptides". *WSEAS Transaction on Biology and Biomedicine*, vol. 12, 2015, pp. 79-86.
- [29] E. Popova, B. Okrugin, I. Neelov, "Molecular Dynamics Simulation of Interaction of Short Lysine Brush and Oppositely Charged Semax Peptides". *Natural Science*, vol. 8, 2016, pp. 499-510.
- [30] D.A. Markelov, S.G. Falkovich, I.M. Neelov, M.Yu. Ilyash, V.V. Matveev, E. Lahderanta, P. Ingman, A.A. Darinskii, "Molecular dynamics simulation of spin-lattice NMR relaxation in poly-L-lysine dendrimers. Manifestation of the semiflexibility effect". *Physical Chemistry and Chemical Physics*, vol. 17, 2015, pp. 3214–3226.
- [31] O.V. Shavykin, I.M. Neelov, A.A. Darinskii, "Is the manifestation of the local dynamics in the spin-lattice NMR relaxation in dendrimers sensitive to excluded volume interactions?", *Physical Chemistry and Chemical Physics*, vol. 18, 2016, pp. 24307-24317.
- [32] I. Neelov, E. Popova, "Complexes of Lysine Dendrimer of 2nd/3rd Generations and Semax Peptides. Molecular Dynamics Simulation". *WSEAS Transaction on Biology and Biomedicine*, vol.14, 2017, pp. 75-82.
- [33] B. Okrugin, I. Neelov, O. Borisov, F. Leermakers, "Structure of asymmetrical peptide dendrimers: insights given by self-consistent field theory", *Polymer*, vol.125, 2017, pp. 292-302.
- [34] I. Neelov, E. Popova. "Molecular Dynamics Simulation of Complex Formation by Lysine Dendrigraft of Second Generation and Semax Peptide," *International J. of Materials*, vol. 4, 2017, pp. 16-21.
- [35] Sadovnichy V., Tikhonravov A., Voevodin V., Opanasenko V. *Contemporary high performance computing: From petascale toward exascale*. Eds. Boca Raton, USA, 2013, pp. 283–307.